Chapter 1

Heat Exchange Analysis on Latent Heat Thermal Energy Storage Systems Using Molten Salts and Nanoparticles as Phase Change Materials

Adio Miliozzi, Raffaele Liberatore, Daniele Nicolini,
Manila Chieruzzi, Elisabetta Veca,
Tommaso Crescenzi and Luigi Torre

Additional information is available at the end of the chapter

http://dx.doi.org/10.5772/intechopen.73672

Abstract

The increase of carbon dioxide emissions is the most important contributor to climate change. A better use of produced energy, increasing systems efficiency and using renewable sources, can limit them. A key technological issue is to integrate a thermal energy storage (TES). It consists in stocking thermal energy through the heating/cooling of a storage material for future needs. Among various technologies, latent heat TES (LHTES) provides high energy storage density at constant temperature during melting/solidification of storage media. The bottleneck in the use of typical PCMs is their low thermal conductivity. To improve the heat exchange between heat transfer fluid and PCM, three methods are possible and here experimentally analyzed: conductivity systems enhancements; convective flows promotion in liquid phase; and improvement of PCM thermal properties including small amounts of nanoparticles. CFD models were used to evaluate physical phenomena that are crucial for optimized LHTES systems design. The study of the heat exchange mode allowed some useful indications to achieve an optimized LHTES, taking advantage by convective flows and conductivity promotion systems. The use of NEPCM, to maximize the stored energy density and realize compact systems, makes necessary the improvement of its thermal diffusivity. These will be the future research topics.

Keywords: heat exchange, latent heat, nanoparticles, phase change material, thermal energy storage

1. Introduction

The increased world energy demand is the most important contributor to climate change. A better use of the produced energy, by increasing the energy efficiency in industrial and civil applications, as well as the use of renewable sources, such as solar energy, can limit the carbon dioxide emissions and, consequently, the man-made greenhouse effect [1]. European Commission introduced in October 2014 new and ambitious targets for the year 2030 [2, 3]: 27% share for renewable energy penetration, 40% cuts in greenhouse gas (GHG) emissions, and 27% improvement in energy efficiency.

A key technological issue to reach these objectives is to integrate in the productive system an efficient and low-cost thermal energy storage (TES) [4, 5]. Thermal energy storage is a technology that consists in stocking thermal energy through the heating and cooling of a storage material. The energy stored in this way can be used for future needs in particular to face the fluctuating energy demand, increasing the efficiency of several systems. The heat can be stored in a heat storage material (HSM) in three different modes: as sensible heat (HSM temperature increasing), as latent heat (HSM phase change, i.e. solid-liquid), or as thermochemical energy (reversible thermochemical reactions).

Among these technologies, latent heat thermal energy storage (LHTES) provides, due to the high absorbed/released energy required by the phase change process of the material, a high-energy storage density at an almost constant temperature during the melting and the solidification of the storage media. These materials are called phase change materials (PCMs). However, in practice, in the place of a single temperature, the system operates in a temperature range, which includes the melting temperature. A PCM can store higher amount of heat if in comparison with a material using only sensible heat, and this leads to a significant decrease of the size and cost of the LHTES systems [6, 7].

PCMs are commonly used in applications for both thermal management and thermal energy storage. For example, LHTES systems can find application [7] in:

- small and large size solar thermal power plants, where the constant temperature of the supplied heat allows a more efficient operation of the gas turbine;
- in industrial plants, where the process heat, deriving from renewable sources, is provided at the required temperature allowing a wide range of processes: food (30–120°C), beverages (60–90°C), paper Industry (60–150°C), metal surface treatment (30–80°C), bricks and blocks curing (60–140°C), textile industry (40–180°C), chemical industry (60–260°C), plastic industry (60–220°C), and other industrial sectors (30–180°C).
- in district heating, industrial cooling, or waste heat recovering.

Typical HSM for medium-high applications are salts or mixtures thereof [8, 9]. The bottleneck of these PCMs is their low thermal conductivity which, combined with a high thermal capacity, leads to a low thermal diffusivity and, therefore, a low exploitation of the material, high

charging times, and low released power. The enhancement of the thermal conductivity of the PCMs is one of the most important topics in LHTES system design. Many development activities, indeed, are focused on this topic with the aim of creating materials with high latent heat, high specific heat, and high thermal conductivity.

To improve the heat exchange between the heat transfer fluid (HTF) and PCM, three methods deserve to be cited [10]:

i. Increase of the heat exchange surface through the introduction of suitable thermal conductivity promotion systems;

ii. Increase of the heat exchange coefficient by exploiting the development of convective flows inside the PCM during the solid-liquid phase change (convective thermal exchange);

iii. Increase the thermal conductivity of HSM by altering its properties through the introduction of small amounts of proper nanoparticles (nanoenhanced PCM (NEPCM)).

The effect of these solutions on heat transfer mode should be carefully analyzed to assess the advantages and disadvantages.

In the first part of this chapter, the commonly used storage media and the methods of increasing the conductivity will be illustrated. Subsequently, some experimental tests will be described, and the results discussed. Finally, after analyzing the numerical methodologies useful to simulate the highlighted physical phenomena, future steps for the development of innovative latent heat storage systems will be described.

2. Heat storage materials

The most common HSMs for medium-high applications are solar salts and their mixtures. They shows good thermal properties and low cost. **Table 1** summarizes some of these HSMs.

It was demonstrated that the main thermal properties of PCMs (in particular in the solar salts) can be enhanced with the addition of several kind of nanoparticles. Some of these properties are latent heat, specific heat, and thermal conductivity. In particular in this paragraph, it is reported how the enhancement of thermal properties is strictly related to some factors like the size, the type, and the weight percentage of nanoparticles, as well as synthesis protocol and the parameters used. For example, nanoparticles with a too little diameter may precipitate instead of dispersing in the liquid or a too high weight percentage can be responsible for a difficult nanoparticle dispersion.

As for the synthesis protocols, the NEPCM can be obtained with several experimental procedures. The most used is the two-step liquid solution method which involves the production of a solution and the use of ultrasound. In particular, in this case, the NEPCMs are prepared by dissolving 200 mg of salt and nanoparticles in solid state (as powder) into 20 ml of distilled water. The dispersion of the nanoparticles is ensured by the ultrasonication of the solution followed by water evaporation on hot plate.

Composition	Melting temp, °C	Latent heat, J/g	Composition	Melting temp, °C	Latent heat, J/g
$LiNO_3$:KNO_3 33:67 [a]	0133	170	NaOH:NaCl:Na_2CO_3 86:8:6 [b]	298	286
KNO_3:$NaNO_2$:$NaNO_3$ 53:40:7 [a]	142	80	$NaNO_3$	307	183
$LiNO_3$:$NaNO_3$ 49:51 [a]	194	265	KNO_3	337	100
$LiNO_3$:NaCl 87:13 [a]	208	369	LiCl:KCl 58:42 [b]	348	170
$NaNO_3$:KNO_3 54:46 [a]	222	110	$MgCl_2$:NaCl:KCl 63:23:24 [a]	385	461
$NaNO_2$:NaOH 80:20 [b]	232	252	KCl:$MgCl_2$:NaCl 20:50:30 [b]	396	291
NaOH:$NaNO_2$ 73:27 [b]	237	272	Li_2CO_3:K_2CO_3:Na_2CO_3 31:35:34 [a]	397	275
NaOH:$NaNO_3$ 28:72 [b]	246	225	LiF:LiOH 80:20 [b]	430	528
$LiNO_3$	253	363	Li:NaF:KF 29:12:59 [a]	463	442
$LiNO_3$:NaCl 93.6:6.4 [a]	255	354	Li_2CO_3:K_2CO_3 47:53 [a]	488	342
LiCl:LiOH 37:63 [a]	262	485	$CaCl_2$:NaCl 55:45 [b]	495	236
$NaNO_3$:NaOH 41:59 [b]	266	278	Na_2CO_3:Li_2CO_3 56:44 [a]	496	368
LiCl:$Ca(NO_3)_2$ 59:41 [b]	270	167	NaCl:$CaCl_2$ 33:67 [a]	500	281
$NaNO_3$-2NaOH [b]	270	295	K_2CO_3:NaF:KCl 62:17:21 [a]	520	274
LiOH:LiCl:KCl 62:36.5:1.5 [b]	282	300	Li_2CO_3:Na_2CO_3:K_2CO_3 22:16:62 [a]	580	288

[a]wt.%.
[b]mol.%.

Table 1. Main properties for some HSMs used as PCMs [11–14].

In general, a sonication is made by using sound energy to disperse particles into a material. When the ultrasonic frequencies are used, the process is called ultra-sonication. The aim of this method is to obtain a uniform dispersion of the nanoparticles, thus avoiding the formation of agglomerates (i.e., clusters of hundreds of single nanoparticles).

Different sonication times (100 and 200 min) and evaporation temperatures (60, 100, and 200°C) can be used in this procedure [15–17].

The typical salts used as PCMs in LHTES are nitrates, at medium-high temperatures (due to their melting temperature which is between 200 and 400°C), and carbonates and chlorides, at high temperatures (since their melting temperature is above 400°C). For example, the dispersion of 1 wt.% of SiO_2 nanoparticles into a mixture of Li_2CO_3 and K_2CO_3 (62:38) with a melting point of 488°C was done under sonication for 100 min followed by water evaporation at 200°C [15]. Above the melting point (in the range 525–555°C), the specific heat of the NEPCM is enhanced by 19–24%. The enhancement was attributed to the formation of a substructure close to the nanoparticles and to the high specific surface energy of the nanoparticles. By increasing the nanoparticles, percentage (1.5 wt.% instead of 1 wt.%) of the same

nanoparticles into the same molten salt mixture different results can be obtained by changing the protocol parameters [16, 17]. In particular, with 200 min and 60°C, a specific heat increase of 34% in solid phase and 101% in liquid phase can be achieved. The morphology of the NEPCMs is characterized by the formation of needle-like structures of nanoparticles in the salt mixture. These structures could be responsible of the specific heat enhancement. Moreover, slow water evaporation (i.e. at lower temperature) seems to be more effective in increasing the specific heat of the salt due to the reduced presence of agglomerates. Other kind of nanoparticles can also be used. A low amount of graphite nanoparticles (0.1 wt.%) added into the same eutectic salt (Li_2CO_3: K_2CO_3 62:38) may produce an increase of the specific heat of 40 and 57% in solid and liquid phase, respectively [18]. Chloride salts and their eutectic mixtures can also be used as HSM at high temperature. An eutectic mixture of barium chloride, sodium chloride, calcium chloride, and lithium chloride ($BaCl_2$:NaCl:$CaCl_2$:LiCl 34.59:12.52:40:12.89) has a melting point of 378°C. The addition of 1 wt.% of SiO_2 nanoparticles to this mixture showed an increase of the specific heat of about 14.5% [19].

The nanoparticle size can also affect the thermal behavior of molten salts and nanoparticles. It seems that higher specific heat increase is obtained with higher nanoparticle diameter. This trend was shown by studying nanofluids based on the common binary nitrate salt of $NaNO_3$:KNO_3 (60:40) having a melting temperature of about 225°C by using the two-step liquid solution method. Lu and Huang [20] used Al_2O_3 nanoparticles with 13 and 90 nm diameter, while Dudda and Shin [21] used SiO_2 nanoparticles (1 wt.%) with 5, 10, 30, and 60 nm in diameter. The possible explanation of this effect is that nanoparticles with little diameter (<10 nm) tend to precipitate or form agglomerates, thus preventing a good dispersion into the molten salt, which is a fundamental step to achieve thermal properties enhancement.

Several experimental studies have been conducted by University of Perugia and ENEA in order to develop NEPCM as HSMs. In one of these [22], SiO_2, Al_2O_3, TiO_2, and a mixture of SiO_2-Al_2O_3 nanoparticles (82–86% silica, 14–18% alumina) were added to the salt mixture $NaNO_3$-KNO_3 (60:40). The NEPCMs were obtained by the two-step liquid solution method described above with 100 min of dispersion and water evaporation at 200°C.

Some considerations could be found. First of all, the NEPCMs showed the highest improvement of the specific heat with 1 wt.% of nanoparticles added, while 0.5 and 1.5 wt.% were not considered effective. Second, the type of nanoparticle played an important role: TiO_2 did not increase the Cp of nitrate salts, while SiO_2 Al_2O_3 showed the greatest enhancement (+22 and +57% in solid and liquid state). Since no substructure was formed in this case, the observed enhancement of heat capacity was attributed to the formation of a solid-like nanolayer on the surface of the nanoparticle.

In a recent study, another HSM was developed through water solution method by using KNO_3 as molten salt (melting point of 334°C) and 1 wt.% of SiO_2, Al_2O_3, and a mixture of SiO_2-Al_2O_3 as nanoparticles [23]. The HSM has an increased specific heat with silica and silica-alumina nanoparticles (+9.5% and +4.7%, respectively). In any case, the two-step method involves the use of high amount of water and the evaporation of the water can be expensive and time consuming. In other words, in industrial scale, it should be tried to produce NEPCMs with easier methods. Few studies report the production of nanofluids based on molten salt and

nanoparticles without water by mixing them with the ball milling procedure (i.e., directly in solid state). In this study [24], a ball-mill with 9 mm stainless steel bearing was used to mix the powder salts and the nanoparticles (CuO and TiO_2). With this procedure and materials, the NEPCMs obtained showed higher latent heat (+2.4 and +3.8%) and specific heat.

Recently, a new mixing methodology was developed by University of Perugia and ENEA [25]. This technique does not involve the use of water, since salts and nanoparticles are mixed together directly at high temperature (i.e., in liquid state). $NaNO_3$:KNO_3 (60:40) and 1.0 wt% of nanoparticles (silica, alumina and a mixture of silica/alumina as above) were mixed together in powder and then heated above the melting temperature (at 300°C) by using a twin screw microcompounder (**Figure 1**). The presence of a recirculating channel ensures the recycling of the NEPCM and the good dispersion of nanoparticles. The materials were mixed at screw speed of 100 and 200 rpm, for 15 and 30 min. After this heating, the mixture is then cooled down at room temperature and ground to powder. The thermal properties of the NEPCMs produced in this way depend on the type of nanoparticle and the time and speed used to mix them. A good HSM was obtained with silica/alumina nanoparticles mixed for 30 min at 200 rpm, reaching a high increase of C_p (+52.1% in solid phase and +18.6% in liquid phase) and good increase of the heat of fusion (+4.7%). The thermal storage capability of molten salts and nanoparticles can be also calculated and evaluated as the integration of the heat flow curve between the minimum and maximum working temperatures. The stored heat was found to enhance by 13.5%.

Another important property of the HSM is their latent heat. The advantage of the increase of latent heat is the increased storage heat capability of the material per unit volume. About the latent heat enhancement, there is lack of information. However, some studies performed by University of Perugia reported an increase of 15% mainly with silica-alumina nanoparticles in nitrate mixture [22] and also in KNO_3 as molten salt having a melting point of 334°C (the latent heat increased by 12%). In both studies, the NEPCMs were produced in water solution [23]. It was shown that the stored heat of molten salts as $NaNO_3$-KNO_3 [22] and KNO_3 [23] is increased with the addition of 1.0 wt.% of SiO_2-Al_2O_3 and SiO_2.

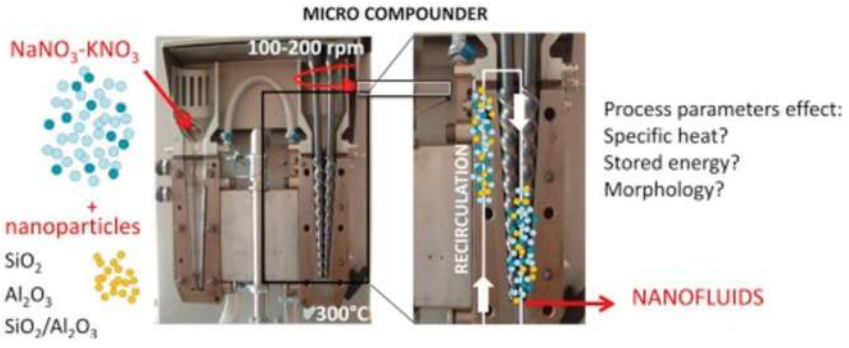

Figure 1. Mixing of nanoparticles and the salt mixture at high temperature in a twin screw microcompounder [21].

Another fundamental property of heat storage materials is their thermal conductivity. However, for many PCMs (especially molten salts), it needs to be increased. Thus, the main idea to increase this property is to combine these PCMs with highly conductive nanomaterials [26]. The research on other nanofluids is wide, but only few studies were performed in particular on molten salts with nanoparticles to enhance the thermal conductivity of the pure materials. One of these showed that only 1 wt.% of SiO_2 nanoparticles may enhance the thermal conductivity of the eutectic mixture of carbonates (Li_2CO_3:K_2CO_3 62:38) by 47% at 150°C and 37% at 300°C with respect to the base salt and the thermal diffusivity by 28 and 25% at 150 and 300°C, respectively [27]. The formation of a percolation network was considered responsible of the enhancement of the thermal conductivity and diffusivity of the nanocomposite (as previously reported about the specific heat enhancement). Recently, University of Perugia [28] produced NEPCMs starting from the nitrate mixture ($NaNO_3$:KNO_3 60:40). Only 1.0 wt.% of silica-alumina nanoparticles (82–86% silica, 14–18% alumina) were dispersed into the salt mixture in a concentrated water solution (from 100 to 500 g/l). The salts and the nanoparticles were mixed by a mechanical stirrer, and the NEPCMs produced showed a higher thermal conductivity value in comparison to the base salt mixture (up to +25%). Moreover, it increased by increasing the aqueous solution concentration (from 100 to 500 g/l), as well as thermal diffusivity (up to +47%).

3. Enhancement of heat exchange in LHTES

The improvement of thermal exchange between heat transfer fluid and PCM is one of the main themes in development of LHTES systems [29]. Commonly, used PCMs show a low conductivity of 0.5–1 W/m K. Therefore, the design of the heat exchanger is dominated by the task to identify effective solutions to increase the equivalent thermal conductivity within the heat storage material [30]. In the previous paragraph, the possibility to act on the material itself by altering its thermal properties by adding small amounts of nanoparticles (NEPCM) was evaluated. In this section, however, two other methods to increase the apparent conductivity of the thermal storage medium were analyzed: introducing a system to promote the conductivity and favoring a convective heat exchange in the liquid phase of PCM.

3.1. Promoting thermal conductivity

Different solutions can be applied to promote thermal conductivity or to improve heat exchange and increase power level [11, 31]:

- Increasing of heat transfer area: the contact area of the heat exchanger between HTF and PCM is enlarged to reduce the average distance for heat diffusion within the PCM. Possible implementations of this approach can use either finned tubes or capsules;
- Composite material with increased thermal conductivity: a material showing a high thermal conductivity is added to the PCM. The PCM can be infiltrated in a porous matrix made up of the additional material, or the two components can be mixed as powders, fibers, or small particles;

- Intermediate heat transfer medium liquid/gaseous: the PCM and a heat exchanger are arranged in a container filled with a medium that transfers the energy between these two components. The heat transport involves the phase change of the heat transfer medium.

A **sandwich structure** is an approach to increase the effective thermal conductivity of the PCM, integrating highly conductive materials layers inside the PCM. The layers are arranged in the heat transport direction (**Figure 2a**). The application of tubes with wings embedded in a PCM is described as a sandwich concept. This concept has been developed, since it seems to be the most promising option for making efficient and low-cost latent heat storage systems [11, 12, 32].

The choice of steel would be a simple solution as well as finned steel tubes are standard components for heat exchangers. Instead, graphite or aluminum sheets are chosen as materials for wings due to their high thermal conductivity. To obtain the same heat transfer performance in comparison with the graphite or aluminum fins, the steel fins require a higher volume and, therefore, significantly higher costs, also due to the higher density (**Table 2**). The costs are proportional to the c/λ factor, where λ is the thermal conductivity and c is the volume specific cost of the fins material.

Mounting the fins on the pipes is a key issue for the sandwich concept. If the material of the fins is different from the material of the pipes two other phenomena can occur: a different thermal expansion between the used materials and a galvanic corrosion (the damage induced when two dissimilar materials are coupled in a corrosive electrolyte). In addition, the application of fins made of expanded graphite offers several advantages beyond a good thermal conductivity. Expanded graphite has good chemical stability with nitrates and nitrites at temperatures up to 250°C, and galvanic corrosion does not occur when it is in contact with steel tubes. Because graphite laminae exhibit a high degree of flexibility and they are often used as a sealing material, a tight contact between the tubes and the fins can easily be achieved [32]. The highest specific price, compared to stainless or carbon steel, is largely compensated by its low density and high thermal conductivity. However, graphite is stable with nitrates only below 250°C. For higher temperature applications, the use of metallic fins is necessary [11]. **Figure 2b** shows semiindustrial applications of this concept.

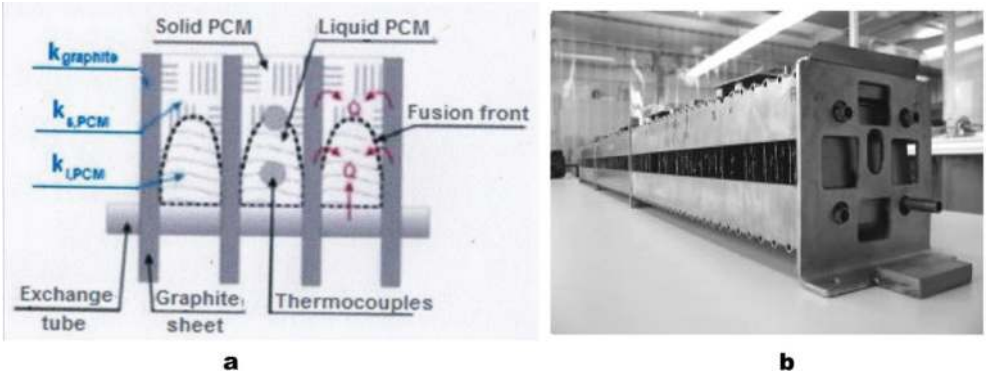

Figure 2. Functional scheme and test module of the LHTES sandwich concept [29, 31, 32].

	Graphite foil	Aluminum	Stainless steel	Carbon steel	Copper
Thermal conductivity λ (W/m K)	150	200	20	30	350
Density ρ (kg/m^3)	1000	2700	7800	7800	8800
Estimated volume specific costs c (€/m^3)	10,000	7000	20,000	15,000	40,000
Estimated c/λ (€K/W m^2)	66.7	35.0	1000	500	114.3

Table 2. Main properties for materials used in LHTES sandwich systems [31, 32].

A second solution is to pack the PCM into capsules in order to reduce the maximum distance for heat transfer or to increase the heat exchange area: this concept is called **macroencapsulation** of the storage medium [11]. **Figure 3** shows an example of LHTES with macrocapsules used in a laboratory scale experiment. In this case, the cylindrical capsules have a length of 0.5 m and a diameter of 15–25 mm and they are filled with a $NaNO_3$-KNO_3 eutectic mixture. The capsules are arranged in parallel and integrated inside a tank. Due to PCM specific volume variations that can reach up to 10% during phase change, the tubes are not fully filled. A volumetric gas fraction of about 20% is required within the rigid capsules to limit the increase in pressure during PCM melting.

Because of the corrosive behavior of some PCM salts, it is necessary to provide a certain minimum thickness of the wall and avoid a flexible encapsulation. However, this concept is not considered a promising solution due, in particular, to some economic aspects and the following disadvantages [11]:

- The amount of material required for pressure capsules is significant, if steel is used: the steel mass is almost equivalent to the mass of PCM;
- The volume fraction of PCM in the pressure tank may be less than 40%;
- The filling and sealing procedure with molten PCM are complex;
- HTF contamination with PCM should be avoided due to leakage from the capsules: this requires high standards of quality with consequent further increase in costs.

Thermal conductivity can also be improved by using **composite materials** in which the properties of a high latent heat of a PCM are combined with that of a good thermal conductivity of an additive. Said composite materials are manufactured in blocks and subsequently assembled together with the tube assembly (**Figure 4**).

If the operational temperature range is 120–300°C, nitrates or nitrites and various types of graphite are currently being used. Graphite was chosen because of its high thermal conductivity and chemical stability. The objective is generally to obtain a composite material with an effective thermal conductivity in the range of 5–15 W/m K using a small amount of graphite to obtain a high capacity and a low cost of the LHTES system. The fraction of graphite mass significantly influences the effective thermal conductivity. The composite material is

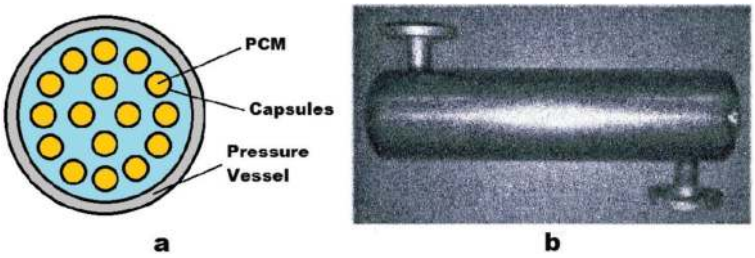

Figure 3. PCM capsules array and external containers [12, 31].

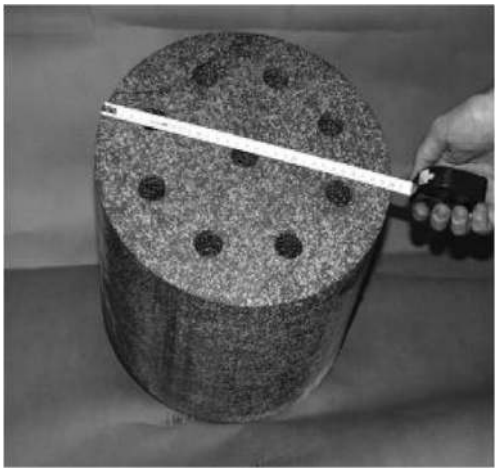

Figure 4. Example of composite material (expanded graphite) with PCM in a laboratory scale element [29, 31].

produced by compression of PCM powders and expanded graphite. The development of an efficient HSM requires the limitation of graphite content because of material costs (ratio of specific expanded graphite/PCM costs is about 20:1) and the reduction in volumetric storage capacity. An important aspect is also the cyclic behavior of composite material. The separation of the components must not be the result of repeated charge/discharge. Indeed, during some experiments, described in literature [11], significant PCM loss occurred, about 40% of nitrate salt separated from graphite. There are several possible causes for the salt loss of the storage module. These causes include the requirement for an empty volume for salt expansion, degassing caused by impurities and moisture in the salts, and poor testability of alkaline metal nitrate salts on graphite and their good wettability on metallic surfaces (tendency to the sliding). Probably, the salt leakage was caused by a combination of these critical phenomena.

3.2. Convective heat exchange

The heat transfer efficiency between the HTF and PCM strongly affects the performance of the charging/discharging cycles of an LHTES system, especially during melting/solidification

phases. During melting, the PCM has to be heated by the HTF (charge process), the heat flows toward the PCM by conduction and later by natural convection. The solid PCM near the heat exchanger surface heats up and then starts to melt, and the thickness of the liquid region increases over time at fluid-solid interfaces. As the thermal conductivity of liquid PCM is less than that of solid PCM, the heat transfer by conduction becomes almost negligible as the melting process moves forward, and the movement of the fluid in terms of convection must also be taken into consideration.

Convective flows are a result of the varying density of the PCM in function of temperature. The whole mass of fluid is subject to a downward gravitational pull. Consequently, lighter portions of fluid will be subject to Archimedes' upward buoyant force. The nonhomogeneity in temperature causes the same in density [10]. The heat transfer to the PCM followed three regimes [33]: conduction; mixed conduction and convection, where conduction domination was gradually replaced by convection when a sufficiently large amount of liquid had formed; and convection. Regarding solidification, the HTF must be heated. A solid layer was produced on the surface of the heat exchanger on the PCM side that affected the heat transfer by conduction. This is the reason why it is important to enhance the thermal conductivity of the LHTES system. The transition from a conductive to a convective regime produced a significant increase in thermal exchange with a reduction in charging and discharging times and consequent increase in available thermal power and system efficiency. The conditions necessary to establish these convective motions have been extensively studied both experimentally [30, 34–36] and numerically [37–41]. The last goal is to promote this sort of heat exchange within the LHTES to achieve an optimized and efficient system.

A preliminary experimental test of PCM melting was performed in ENEA in a small tubular reactor in a temperature range between 180 and 300°C. The experiment also included the cooling down of the system. Only the time period of the fusion phase was taken into account. The PCM was a mixture of nitrate salts, whose composition is $NaNO_3$-KNO_3 (60:40%wt), the dimensions of the AISI 316 reactor were 66 mm internal diameter, 70 mm external diameter, and 310 mm high. It contained about 2 kg of molten salts, and the tubular reactor was equipped with an external heating element, made in kanthal, placed along the wall. Instrumentation for the acquisition of the temperature and pressure was also present.

There are 18 thermocouples for temperature measurement inside the reactor: they are placed on six planes. Each plane contains three thermocouple tubes positioned at 120 degrees from each other at three different radial distances.

For the melting test, the reactor was loaded with 2 kg of PCM in order to have a uniform composition. The PCM was heated up to 300°C and then cooled down.

- The heating from 180 to 300°C was set without programming any temperature ramp on the controller. This is the reason why it overshoots the desired temperature value.
- During the heating phase, the salts started to melt in the temperature range of 220–240°C. In **Figure 5**, the blue dotted lines correspond to the melting temperature interval, and the blue line is the time of the melting process.

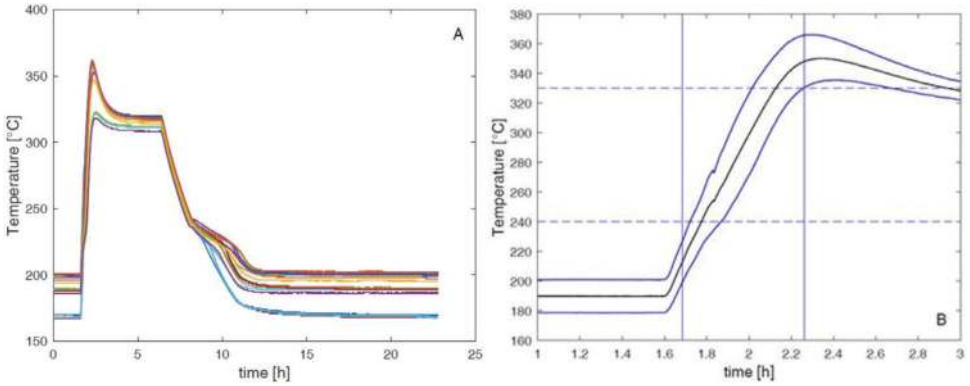

Figure 5. (A) All of the 18 thermocouples over experimental test time; (B) The black line is the mean temperature value; and the blue line is the standard deviation ± σ.

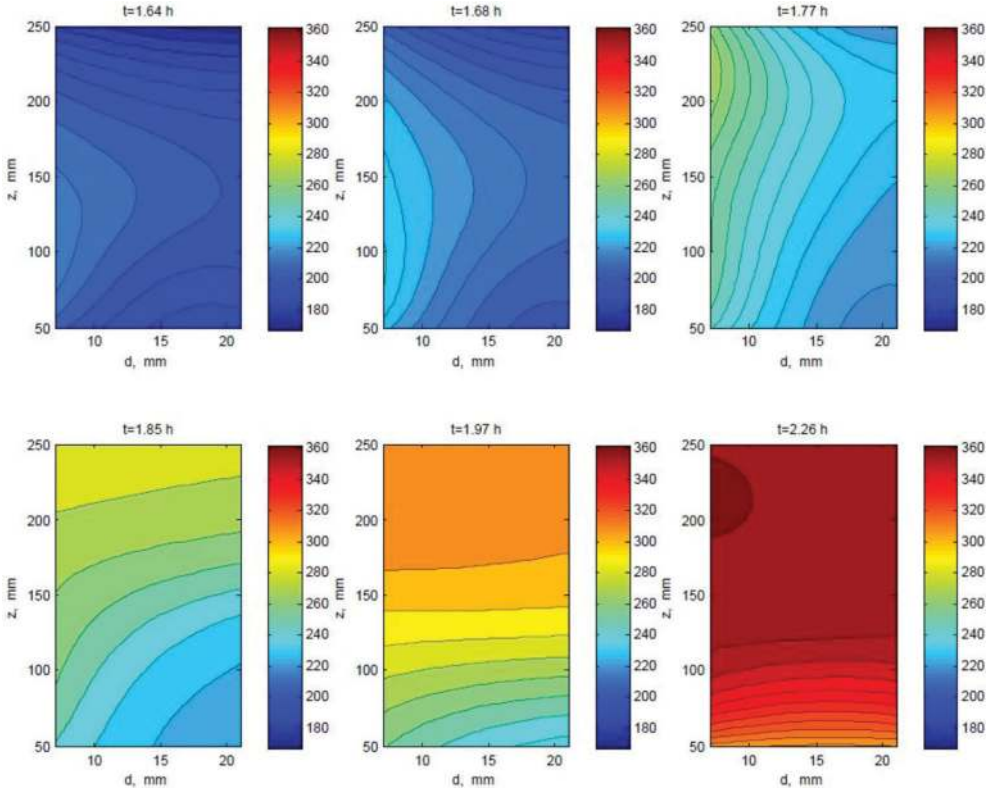

Figure 6. Temperature contour lines inside the reactor for 6 different times during the melting process. d(mm) is the distance from the wall heated by electrical heater and z(mm) is the height.

- Isotherm at 300°C for 3 h 20 min.
- The cooling down of the system from 300 to 180°C was by natural convection at room temperature (after approximately 5 h). During the cooling down phase, the PCM solidified within the same range of temperature.

Only the melting process was taken into consideration, the temperature contour lines inside the reactor are described in **Figure 6**. The melting process started after 1 h 46 min, and all of the experimental temperature data are reported in function of d and z for six different times as the fusion took place. At 1 h 38 min, the PCM was solid, and shortly thereafter, it started to melt; at 1 h 45 min, the solid phase started to collapse. Five minutes later, the solid phase was bound at the bottom right. After 2 h, it was completely liquid and homogenization by convection started, which was in turn induced by internal temperature gradients. At 2 h 15 min, the PCM homogenized by simple conduction with the presence of a convective cell at the top of the reactor. Moreover, the liquid phase pushed the solid downward, and the heat flux is orthogonal to the temperature contour lines.

4. Experimental tests on simple LHTES

An experimental system (**Figure 7a**), whose operating temperature varies in the range 150–300°C, was installed in ENEA CR Casaccia to carry out a cognitive survey of the involved phenomena. It consists of a series of stainless steel cylinders (**Figure 8a**) able to contain about 2.5 l of material, an heating/cooling circulator to handle thermal oil used as transfer fluid to charge and discharge it, four electro-valves to allow different oil circulations, a flow-meter, as well as 32 thermocouples to detect the temperature evolutions. The thermocouples inside the cylinder (**Figure 7b**) were equally spaced both axially and radially in such a way that they have a homogeneous temperature record in order to properly analyze their developments within the material. Eventually, a SW interface, based on LabView®, permits to control the system also in remote. The pipe, where the oil (Therminol 66) flows, together with the cylinder containing it, is a shell and tube type exchanger. In order to study the effect of the exchange surface, the external area of the tube in the cylinder can be plain or finned (**Figure 8b**). These cylinders were then insulated with 10 cm of Rockwool and covered by an aluminum sheet (**Figure 8c**).

A thermocryostat Julabo® HT30M1CU ensures the heating and cooling, as well as the handle of the oil thanks to an integrated centrifugal pump, which allows a volume flow rate up to 11 l/min, ensuring a turbulent flow. This equipment, with a 3 kW heating power and a 15 kW cooling power, is able to heat a thermal fluid up to 400°C, but, in our case, the oil was wormed up to 300°C to avoid its cracking. Four kinds of tests were carried out, each one using three cylinders in series of same type:

1. PCM in the cylinder with plain exchanger tube inside;
2. PCM in the cylinder with finned exchanger tube inside;

3. NEPCM (PCM doped with 1%wt of nanoparticles, 20–200 nm, of SiO_2-Al_2O_3) in the cylinder with plain exchanger tube inside;
4. NEPCM in the cylinder with finned exchanger tube inside;

Every test has been conducted 2–3 times to verify the repeatability of the results. During the tests, the thermocryostat was programmed in order to allow the oil to ensure the following temperature trend, where seven distinct phases can be clearly identified: (a) heating phase from room temperature to 200°C (1 h), (b) maintaining temperature at 200°C (10 h), (c) heating phase from 200 to 280°C (1 h), (d) charging phase at 280°C (8 h), (e) cooling phase from 280 to 150°C, (f) system discharging phase at 150°C (8 h), and finally, (g) cooling phase (4 h). **Figure 9** shows the temperature evolutions in the middle section of a cylinder (**Figure 7b**). In case of test with more cycles, the phases c-d-e-f were replicated (**Figure 10**).

A comparison between tests 1 and 2 points out that, in the test using finned tube as exchanger, the temperature trend of the HTF in the zones near the exchanger (blue line) is closer to the oil in the tube. Thus, it shows a better thermal exchange, surely due to the kind of exchange surface;

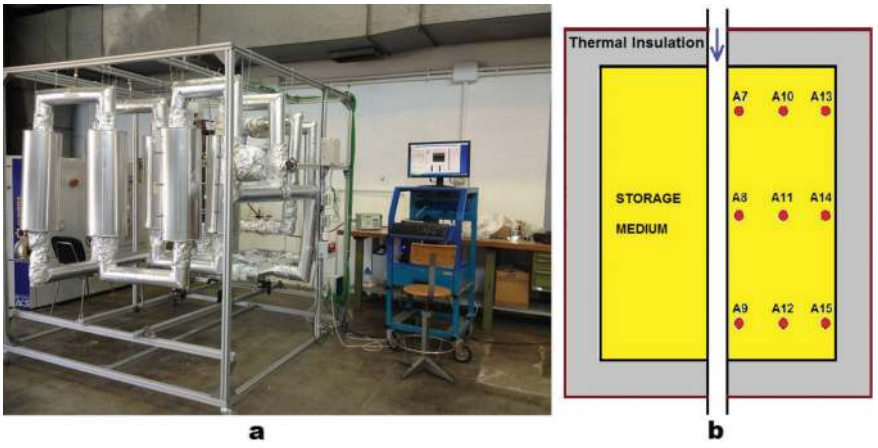

Figure 7. ATES plant (a) and thermocouple positioning inside a reference cylinder (b).

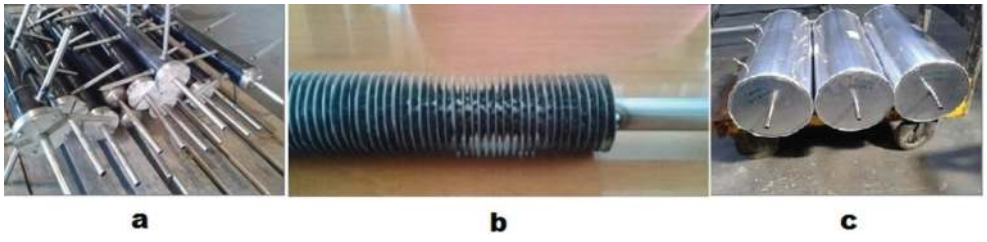

Figure 8. LHTES shell and tube configuration: (a) elementary systems; (b) finned tube; (c) complete systems.

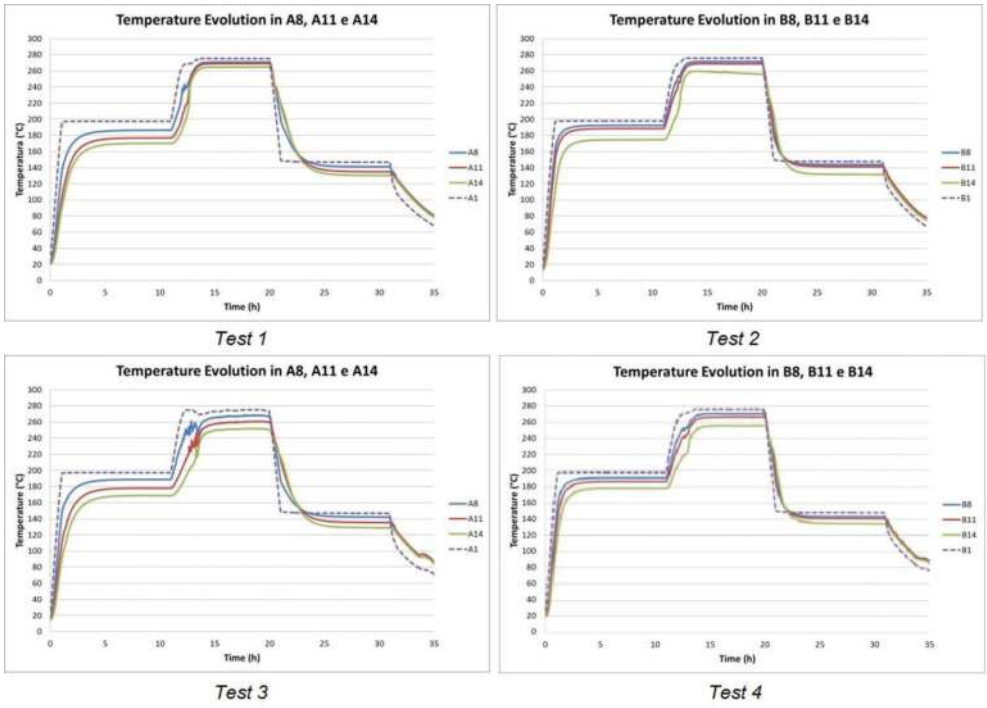

Figure 9. HSM temperatures evolution in the middle section of the first TES [42].

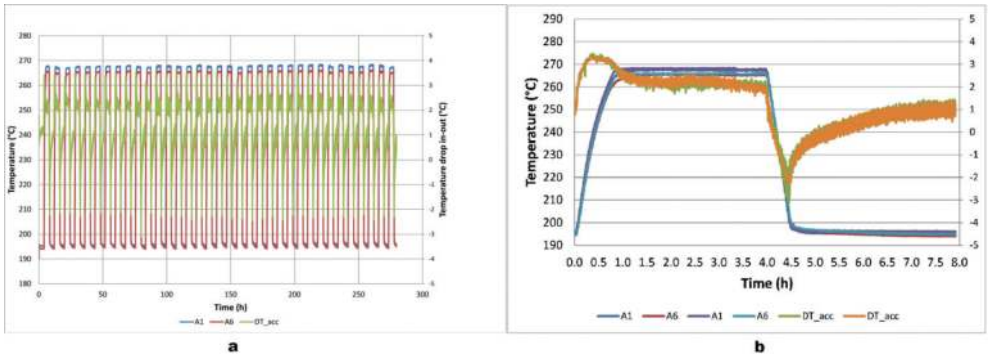

Figure 10. (a) Input (A1) and output (A6) temperature evolution and temperature drop in storage system and (b) temperature in-out HTF and their difference.

nevertheless, the temperature gradient increases, as it goes to the peripheral areas, which means a worse heat absorption within the medium. This phenomenon could be explained also by the Agyenim observations, in fact he claims [9]: "*Phase change problems, first treated as pure conduction controlled, has in recent times moved to a different level of complexity with added convection in the*

melt being accounted for". This phenomenon was not detected, in general, if finned tubes were used (test 2 and 4), probably for the physical limitations of the fins. These convective flows, however, were not found even in the NEPCM with plain exchanger tube, as it can be easily seen by observing test 3, where the green line is more distant from the others than in test 1. In this case, the presence of nanoparticles significantly increases the viscosity [9, 43, 44] of the fluid and probably inhibits the starting of the abovementioned flows [40]. Thus, we can affirm that, when the PCM is in liquid phase and there are no physical limitations (i.e. with plain tubes), the low thermal conductivity (λ) and diffusivity ($\alpha = \lambda(\rho c_p)^{-1}$) are counterbalanced by the start of convective flows thus improving the heat transfer. In NEPCM, despite a substantial invariance of the thermal diffusivity, the thermal capacity and the correlated thermal effusivity, $e = (\lambda \rho c_p)^{1/2}$, are increased. So, in this case, the storage material better exchanges thermal energy with its surroundings (e.g., exchanger) but not inside itself (depending on the diffusivity).The use of finned tubes highlights the promotion of the thermal conductivity, and so the charging and discharging times are lower and substantially independent from the storage medium. It is worth to notice that finned tubes make discharge rate faster because the insulation effect, due to the salt solidification on the wall of the exchanger tube, is compensated by the action of the fins. They in fact improve the thermal exchange for the increased surface. In any case, the TES system with NEPCM and finned tubes through the greater heat capacity, coupled with the lower discharge times, allows the system to deliver a higher average project power.

Cyclability tests (**Figure 10a**) performed on the NEPCM showed the substantial invariance of the storage medium behavior along the cycles. **Figure 10b**, in particular, emphasizes the perfect overlap of the temperature differences between inlets and outlets at 10th and 30th cycle. This makes it well to hope that nanostructured material keeps its features in time.

5. Numerical analysis on LHTES thermal behavior

The correct evaluation of the physical phenomena, that are at the base of the LHTES systems, is crucial for the design of optimized LHTES systems. Since computational fluid dynamics (CFD) models to simulate the thermofluid dynamics behavior of the LHTES system is essential for a good design of these systems, in this section, two models are briefly described. They were developed, by the use of COMSOL Multiphysics® software, ver. 5.2, to simulate the heat storage process for two different geometrical configurations.

Two different geometrical configurations were considered for the LHTES system. In the first one (Model 1), the heat exchange between the heat transfer fluid, oil, and the PCM, "solar salts" ($NaNO_3$-KNO_3), occurs through tubes, whose outer wall is smooth. In the second geometry (Model 2), the tubes have a series of transversal fins on the outer surface, so as to improve the thermal exchange with the PCM. In particular, it was considered a section of steel tube of external diameter of 16 mm, thickness 1 mm, and length 500 mm, surrounded by a tubular crown of PCM of external diameter 70 mm. In the finned configuration, a series of transversal fins of 1 mm thickness and 10 mm height were inserted on the outer surface of the tube and placed at constant interval of 50 mm. Both systems have axial symmetry, and so two 2-D axial symmetry models have been made. Furthermore, since the comparison of the thermofluid

dynamic behavior of PCM is the most important issue, only this material has been simulated. **Figure 11** shows the two models with a mesh detail.

The PCM was modeled as a constant-density fluid, and the buoyancy force was simulated by inserting the vertical component of a volume force equal to $\rho \cdot g \cdot \alpha \cdot (T - T_0)$, where ρ is the density, g is the gravity acceleration, and α is the thermal expansion coefficient at the reference temperature T_0. The phase change condition has been simulated through the use of the liquid fraction (β), defined as: $\beta = 0$ for $T \leq T_{sol}$, $\beta = (T - T_{sol})/(T_{liq} - T_{sol})$ for $T_{sol} < T < T_{liq}$ and $\beta = 1$ for $T \geq T_{liq}$; where T_{sol} is the temperature at which the solid material begins the liquefaction process, and T_{liq} is the temperature at which the material has completed the liquefaction process. The fluid-dynamic behavior of phase change is simulated by inserting the dissipative term $F = [(1-\beta)^2/(\beta^3 + \varepsilon)] \cdot A_{mush} \cdot u$ in the equation of conservation of momentum; where ε is a very small number (0.001), introduced in the equation to avoid division for zero as $\beta = 0$, A_{mush} is the "mushy zone constant", equal to 100,000 kg/(m^{3}s), and u is the velocity of the fluid. The thermodynamic behavior associated with absorption and release of latent heat (L_{fus}) has been simulated by adding, in the transition zone between T_{sol} and T_{liq}, to the specific heat of PCM the term $L_{fus}/(T_{liq} - T_{sol})$. The external walls have been simulated as adiabatic surfaces, while the wall corresponding to the surface of the steel tube has been considered as a temperature-controlled wall in both models. The temperature evolution on this wall provides a first linear rise step, from the initial minimum temperature of 200°C to the maximum temperature of 250°C in 1 h and a subsequent step at the maximum temperature for 3 h. Then, it follows a linear descent ramp from the maximum value to the minimum temperature value in 1 h and a step at the minimum temperature for 3 h. The total time of the simulated test is 8 h. **Figure 12** shows the distributions of liquid fraction of PCM, for both models, at time t = 3900 s, and **Figure 13** shows the velocity in the complete models and in their upper part always at t = 3900 s.

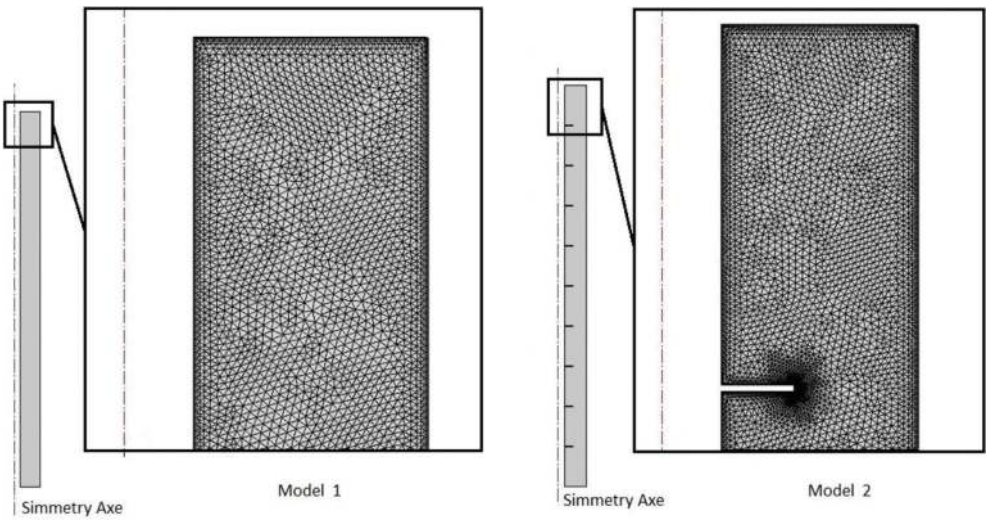

Figure 11. CFD models with a mesh detail.

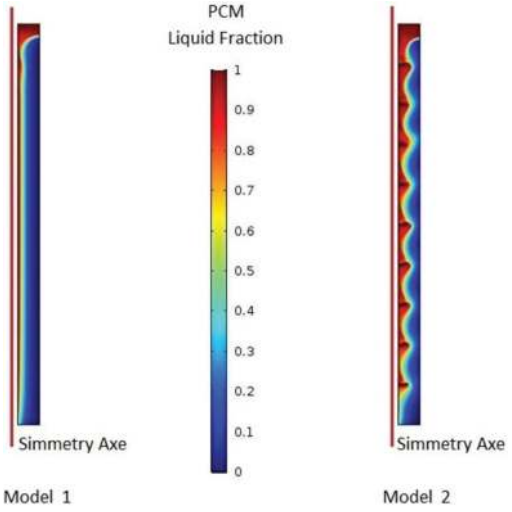

Figure 12. PCM liquid fraction at t = 3900 s.

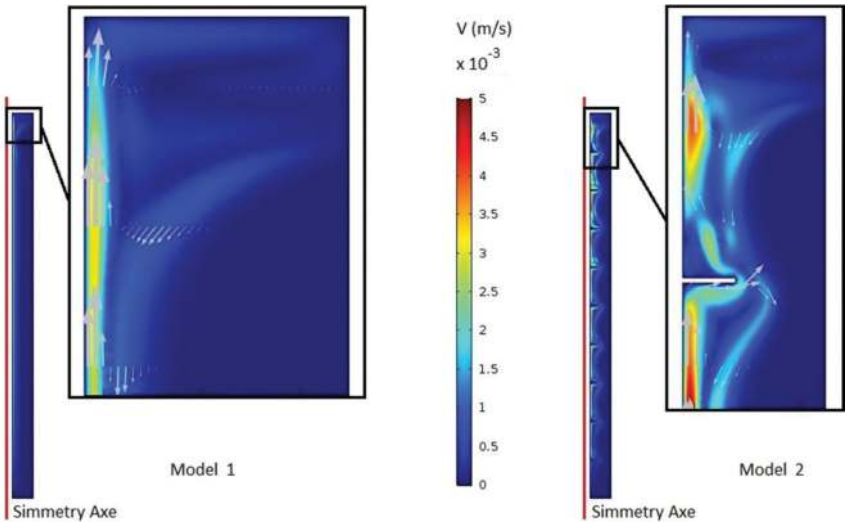

Figure 13. Velocity at t = 3900 s.

Figure 14 shows the comparison between the time evolutions of the melted PCM in the two simulations during the entire charge-discharge cycle. **Figure 15** shows the comparison between the time evolutions of the energy stored by the system in the two models. For comparison, the energy is reported as a percentage of the total energy that can be stored in each of the two systems.

Comparing the results obtained by the two CFD simulations, it is possible to see how the presence of the fins on the outer surface of the steel tube strongly increases the efficiency of the system.

http://dx.doi.org/10.5772/intechopen.73672

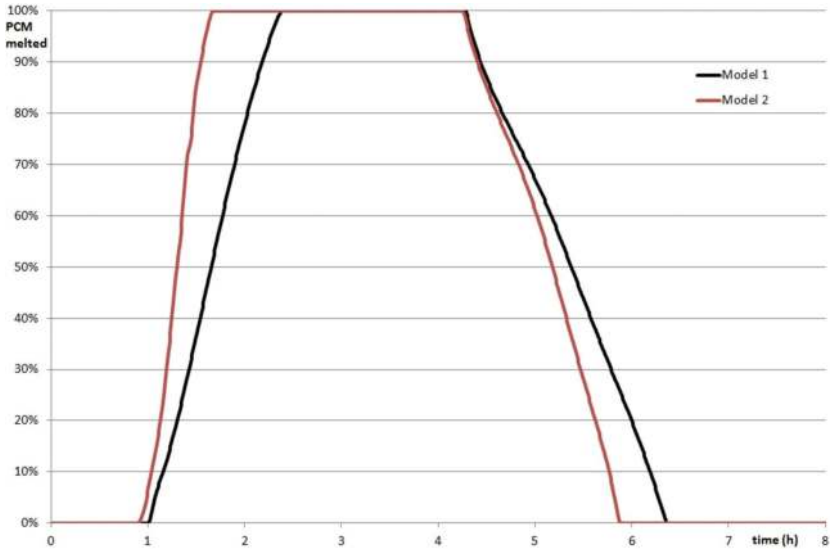

Figure 14. Time evolution of melted PCM.

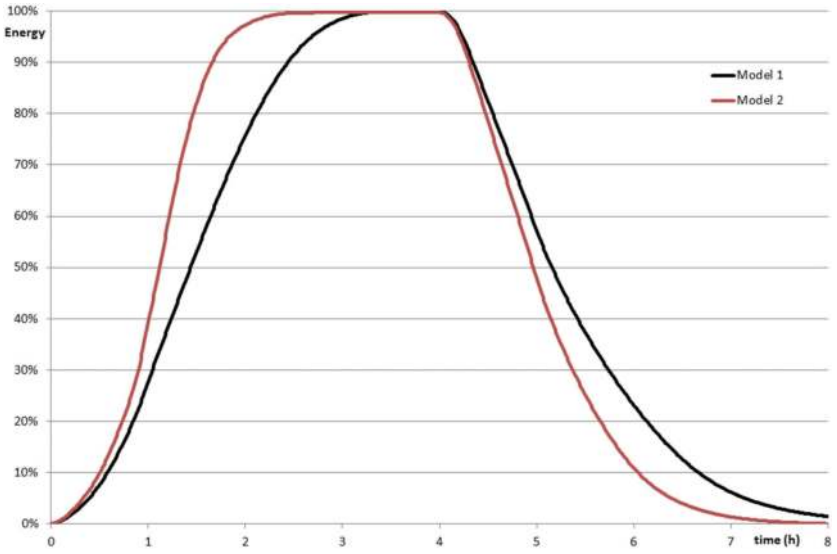

Figure 15. Time evolution of stored energy.

6. Conclusions and future developments

Thermal energy storage is a key technological issue to have an efficient use of the energy and reduce the carbon dioxide emissions and greenhouse effect. Latent heat storage offers

the possibility of designing much smaller TES systems and thus decreasing the cost of stored energy. However, to develop an efficient LHTES system is necessary to select or synthetize an appropriate heat storage material (PCM) with high thermal properties and to increase the HTF-PCM heat exchange, actually limited by the PCM low thermal conductivity/diffusivity. In particular, it is worth to pay attention to the selection of the materials in order to have good thermal properties for storing a large density of energy. For this purpose, a proper synthesis of new PCMs with increased thermal properties by adding little amount of nanoparticles (NEPCMs) can be convenient. In addition, the heat exchange surface plays an important role through the introduction of suitable thermal conductivity promotion systems, and so its design must be well evaluated and optimized, even in the light of the possible exploitation of the development of convective flows inside the PCM during the solid-liquid phase change. Both experimental and theoretical analyses to deepen these phenomena are necessary, and at this purpose, an experimental facility called ATES was developed by ENEA to take into account these phenomena and produce data for elaborating numerical analysis to carefully analyze the advantages and disadvantages of the various solutions and design innovative LHTES systems.

The study on the heat storage materials and heat exchange mode has allowed to obtain some useful indications on the LHTES design and optimization. It should take advantage by the presence of convective flows and conductivity promotion systems to facilitate the heat exchange. Instead, the use of NEPCM as a storage medium, useful to maximize the stored energy density and realize compact systems, makes necessary to improve its thermal diffusivity: this could be done by adding carbon-based nanoparticles to the PCM because they show a high thermal conductivity. Among these, carbon nanotubes (CNTs) and graphene nanoplatelets (GNP) can be used.

These will be the main research topics for the development of new concepts of LHTES.

Acknowledgements

The authors would like to acknowledge the 2014 Annual Research Plan of the Electric System Research Program (RSE) of the Italian Ministry of Economic Development and the EU through the 7th FP in the frame of the STAGE-STE Project (Ctr. Nr. 609837) for the financial support of this work.

Author details

Adio Miliozzi[1]*, Raffaele Liberatore[1], Daniele Nicolini[1], Manila Chieruzzi[2], Elisabetta Veca[1], Tommaso Crescenzi[1] and Luigi Torre[2]

*Address all correspondence to: adio.miliozzi@enea.it

1 ENEA, Italian National Agency for New Technologies, Energy and Sustainable Economic Development, Casaccia Research Centre, Rome, Italy

2 Civil and Environmental Engineering Department, University of Perugia, Terni, Italy

References

[1] Miliozzi A, Liberatore R, Giannuzzi GM, Veca E, Nicolini D, Lanchi M, Chieruzzi M. ENEA research and innovation on Thermal Energy Storage for CSP plants. In: 16th CIRIAF National Congress, Sustainable Development, Human Health and Environmental Protection; April 7-9, 2016; Assisi (Italy). 2016

[2] EU Commission. Climate strategies & targets. 2030 Climate & energy framework. Available from: https://ec.europa.eu/clima/policies/strategies/2030_en [Accessed: Feb 2017]

[3] EU Commission. Climate strategies & targets. 2020 Climate & energy package. Available from: https://ec.europa.eu/clima/policies/strategies/2020_en [Accessed: Feb 2017]

[4] Miliozzi A, Chieruzzi M, Torre L, Kenny JM. Nanofluids with enhanced heat transfer properties for thermal energy storage. In: Tiwari A, Mishra YK, Kobayashi H, Turner APF, editors. Intelligent Nanomaterials. 2nd Ed. Hoboken, NJ, USA: John Wiley & Sons, Inc.; 2016. p. 295-360. ISBN: 978-1-119-24248-2

[5] Salomoni VA, Majorana CE, Giannuzzi GM, Miliozzi A, Nicolini D. New trends in designing parabolic trough solar concentrators and heat storage concrete Systems in Solar Power Plants. In: Rugescu RD, editor. Solar Energy. InTech; 2010. p. 267-292. ISBN: 978-953-307-052-0

[6] Chieruzzi M, Veca E Miliozzi A, Torre L. Phase change materials for latent heat storage: research and future trend. In: 16th CIRIAF National Congress, Sustainable Development, Human Health and Environmental Protection; April 7-9, 2016; Assisi (Italy). 2016

[7] Fleischer AS, editor. Thermal Energy Storage Using Phase Change Materials - Fundamentals and Applications. SpringerBriefs in Applied Sciences and Technology. New York, Dordrecht, London: Springer Heidelberg; 2015. 94 p. DOI: 10.1007/978-3-319-20922-7

[8] Liu M, Saman W, Bruno F. Review on storage materials and thermal performance enhancement techniques for high temperature phase change thermal storage systems. Renewable and Sustainable Energy Reviews. 2012;**16**:2118-2132

[9] Agyenim F, Hewitt N, Eames P, Smyth M. A review of materials, heat transfer and phase change problem formulation for latent heat thermal energy storage systems (LHTESS). Renewable and Sustainable Energy Reviews. 2010;**14**:615-628

[10] Jegadheeswaran S, Pohekar SD. Performance enhancement in latent heat thermal storage system: A review. Renewable and Sustainable Energy Reviews. 2009;**13**:2225-2244

[11] Steinmann WD, Laing D, Tamme R. Latent heat storage systems for solar thermal power plants and process heat applications. Journal of Solar Energy Engineering. 2010;**132**:1-5

[12] Tamme R, Bauer T, Buschle J, Laing D, Muller-Steinhagen H, Steinmann WD. Latent heat storage above 120°C for applications in the industrial process heat sector and solar power generation. International Journal of Energy Research. 2008;**32**:264-271

[13] Michels H, Pitz-Paal R. Cascaded latent heat storage for parabolic trough solar power plants. Solar Energy. 2007;**81**(6):829-837

[14] Kenisarin MM. High-temperature phase change materials for thermal energy storage. Renewable & Sustainable Energy Reviews. 2010;**14**(3):955-970

[15] Shin D, Banerjee D. Enhanced specific heat of silica Nanofluid. Journal of Heat Transfer-Transactions of the Asme. 2011;**133**(2):024501(4 pages)

[16] Shin D, Banerjee D. Enhanced specific heat capacity of Nanomaterials synthesized by dispersing silica nanoparticles in eutectic mixtures. Journal of Heat Transfer-Transactions of the Asme. 2013;**135**(3)

[17] Shin D, Banerjee D. Effects of silica nanoparticles on enhancing the specific heat capacity of carbonate salt eutectic (work in progress). The International Journal of Structural Changes in Solids. 2010;**2**(2):25-31

[18] Jo B, Banerjee D. Enhanced specific heat capacity of molten salt-based nanomaterials: Effects of nanoparticle dispersion and solvent material. Acta Materialia. 2014;**75**:80-91

[19] Shin D, Banerjee D. Enhancement of specific heat capacity of high-temperature silica-nanofluids synthesized in alkali chloride salt eutectics for solar thermal-energy storage applications. International Journal of Heat and Mass Transfer. 2011;**54**(5-6):1064-1070

[20] Lu M, Huang C. Specific heat capacity of molten salt-based alumina nanofluid. Nanoscale Research Letters. 2013;**8**:292(7 pages)

[21] Dudda B, Shin D. Effect of nanoparticle dispersion on specific heat capacity of a binary nitrate salt eutectic for concentrated solar power applications. International Journal of Thermal Sciences. 2013;**69**:37-42

[22] Chieruzzi M, Cerritelli GF, Miliozzi A, Kenny JM. Effect of nanoparticles on heat capacity of nanofluids based on molten salts as PCM for thermal energy storage. Nanoscale Research Letters. 2013;**8**(1):448

[23] Chieruzzi M, Miliozzi A, Crescenzi T, Torre L, New Phase KJMA. Change material based on potassium nitrate with silica and alumina nanoparticles for thermal energy storage. Nanoscale Research Letters. 2015;**10**(1):984

[24] Lasfargues M, Geng Q, Cao H, Ding Y. Mechanical dispersion of nanoparticles and,its effect on the specific heat capacity of impure binary nitrate salt mixtures. Nanomaterials. 2015;**5**(3):1136-1146

[25] Chieruzzi M, Cerritelli GF, Miliozzi A, Kenny JM, Torre L. Heat capacity of nanofluids for solar energy storage produced by dispersing oxide nanoparticles in nitrate salt mixture directly at high temperature. Solar Energy Materials and Solar Cells. 2017;**167**:60-69

[26] Khodadadi JM, Babaei LFH. Thermal conductivity enhancement of nanostructure-based colloidal suspensions utilized as phase change materials for thermal energy storage: A review. Renewable and Sustainable Energy Reviews. 2013;**24**:418-444

[27] Shin D, Banerjee D. Enhanced thermal properties of SiO2 nanocomposite for solar thermal energy storage applications. International Journal of Heat and Mass Transfer. 2015;**84**:898-902

[28] Chieruzzi M, Miliozzi A, Crescenzi T, Kenny JM, Torre L. Synthesis and characterization of nanofluids useful in concentrated solar power plants produced by new mixing methodologies for large-scale production. Journal of Heat Transfer. 2018;**140**(4):042401(13 pages)

[29] Laing D. Storage development for direct steam generation power plants. In: Parabolic Trough Technology Workshop; March 9, 2007, Golden CO, USA. 2007

[30] Fan L, Khodadadi JM. Thermal conductivity enhancement of phase change materials for thermal energy storage: A review. Renewable and Sustainable Energy Reviews. 2011;**15**:24-46

[31] Steinmann WD, Tamme R. Latent heat storage for solar steam systems. Journal of Solar Energy Engineering. 2008;**130**:1-5

[32] Steinmann WD, Laing D, Tamme R. Development of PCM storage for process heat and power generation. Journal of Solar Energy Engineering. 2009;**131**:1-4

[33] Agyenim F, Eames P, Smyth M. A comparison of heat transfer enhancement in a medium temperature thermal energy storage heat exchanger using fins. Solar Energy. 2009;**83**:1509-1520

[34] Agyenim F, Eames P, Smyth M. Experimental study on the melting and solidification behaviour of a medium temperature phase change storage material (Erythritol) system augmented with fins to power a LiBr/H2O absorption cooling system. Renewable Energy. 2011;**36**:108-117

[35] Jones BJ, Sun B, Krishnan S, Garimella SV. Experimental and numerical investigation of melting in a cylinder. International Journal of Heat and Mass Transfer. 2006;**49**:2724-2738

[36] Tan FL. Constrained and unconstrained melting inside a sphere. International Communication of Heat and Mass Transfer. 2008;**35**:466-475

[37] Fornarelli F, Camporeale SM, Fortunato B, Torresi M, Oresta P, Magliocchetti L, Miliozzi A, Santo G. CFD analysis of melting process in a shell-and-tube latent heat storage for concentrated solar power plants. Applied Energy. 2016;**164**:711-722

[38] Guo S, Li H, Zhao J, Li X, Yan J. Numerical simulation study on optimizing charging process of the direct contact mobilized thermal energy storage. Applied Energy. 2013;**112**:1416-1423

[39] Archibold AR, Rahman MM, Goswami DY, Stefanakos EK. The effects of radiative heat transfer during the melting process of a high temperature phase change material confined in a spherical shell. Applied Energy. 2015;**138**:675-684

[40] Sciacovelli A, Gagliardi F, Verda V. Maximization of performance of a PCM latent heat storage system with innovative fins. Applied Energy. 2015;**137**:707-715

[41] Seddegh S, Wang X, Numerical HAD. Investigation of heat transfer mechanism in a vertical shell and tube latent heat energy storage. Applied Thermal Engineering. 2015;**87**:698-706

[42] Miliozzi A, Liberatore R, Crescenzi T, Veca E. Experimental analysis of heat transfer in passive latent heat thermal energy storage systems for CSP plants. Energy Procedia. 2015;**82**:730-736

[43] Goharshadi EK, Ahmadzadeh H, Samiee S, Hadadian M. Nanofluids for heat transfer enhancement–a review. Physical Chemistry Research. 2013;**1**:1-33

[44] Bashirnezhad K, Bazri S, Safaei MR, Goodarzi M, Dahari M, Mahian O, Dalkiliça AS, Wongwises S. Viscosity of nanofluids: A review of recent experimental studies. International Communication of Heat and Mass Transfer. 2016;**73**:114-123. DOI: 10.1016/j.icheatmasstransfer.2016.02.005